CANCELLATION OF FEEDTHROUGH DYNAMICS USING A FORCE-REFLECTING JOYSTICK

R. Brent Gillespie

Department of Mechanical Engineering
Northwestern University
Evanston, Illinois 60208
b-gillespie@nwu.edu

Christopher Hasser

Immersion Corporation
San Jose, California 95131
chasser@immerse.com

Philip Tang

Department of Mechanical Engineering
Northwestern University
Evanston, Illinois 60208

ABSTRACT

This paper reports on a set of theoretical and experimental investigations into the use of force reflection to enhance the dynamic behavior of human piloted vehicles, especially joystick-controlled vehicles such as fly-by-wire jets, bulldozers, and powered wheelchairs. Briefly, force reflection is used in the manual controls to cancel the effects of feedthrough dynamics. Feedthrough dynamics refers to generation of inadvertent steering or speed command inputs due to the action of inertia forces between the pilot's hand and manual controls. These inertia forces arise in the pilot's body in response to vehicle accelerations. To eliminate feedthrough dynamics, a canceling force is produced on the force-reflecting joystick using a model of the pilot dynamics and the known vehicle accelerations. A custom motion platform and a commercial force-reflecting joystick are used in a set of experiments to test the idea. Parameter values for an assumed model are estimated by observing the response of the pilot's body to known platform accelerations. Cancellation of feedthrough dynamics is demonstrated for a human subject.

1 INTRODUCTION

Feedthrough dynamics refers to the effects of inertia forces that arise in the arm and hand of a pilot from accelerations of the vehicle in which the pilot rides. At the mechanical contact between pilot and the manual controls, these inertia forces effectively add to the command forces produced volitionally (through muscle activation) by the pilot. One speaks of the motions of the vehicle "feeding through" and being filtered by the dynamics of the pilot's body to produce extraneous command inputs on the controls. Since the displacements of the manual controls are used in turn to accelerate or steer the vehicle, there exists a control loop that includes the dynamics of the pilot's body but omits the pilot's senses, central nervous system, and muscles. If there exists a significant phase delay between the resulting displacements of the manual controls and the vehicle accelerations that they produce, oscillatory vehicle motion may arise. These oscillations may be sustained or transient, depending on the balance of dissipative and destabilizing effects present in the interactive dynamics. Although a pilot may attempt to correct the oscillatory behavior by applying voluntary muscle control, such efforts may actually aggravate the effect rather than correct for it, due to inherent neuro-motor control delays.

Feedthrough dynamics does not usually play a role in vehicles with steering wheels, since the axis of the steering wheel is orthogonal to the angular accelerations produced by steering. However, feedthrough dynamics plays a significant role in the behavior of many joystick-controlled vehicles. The oscillatory fore and aft motion known as "bucking" in powered wheelchairs is an example (Banerjee et al., 1996). In high-performance fly-by-wire jets, a transient oscillatory motion called "roll ratcheting" often occurs at the end of roll maneuvers (Smith and Montgomery, 1996). The destabilizing effects of feedthrough dynamics can be particularly dangerous in joystick-controlled earth-moving vehicles, such as bulldozers, for the parameters of the pilot-vehicle system change not only each time a new pilot sits in the vehicle but also each time the vehicle picks up or deposits a load. Although the interactive dynamics may be stable for one set of parameters, it may be unstable for another. Often the sustained oscillations will continue to grow in amplitude until the pilot takes his hand off the joystick or the load falls off the vehicle.

Our strategy for canceling feedthrough dynamics is quite simple. The joystick is motorized so that a force may be produced that opposes the inertia force applied to the joystick by the pilot's hand. The joystick-produced force is intended to balance the inertia force, effectively canceling the effects of feedthrough dynamics. Production of such forces on the joystick is based on the known or tracked motion of the vehicle and a dynamical model of the human pilot.

With a dynamical model of the arm as it is coupled to the vehicle chair (through the shoulder and torso) and to the joystick (through the hand), we can estimate the force that will be applied

to the joystick when the chair accelerates and the human exerts no volitional control. We call this the feedthrough force. We assume that the force applied to the joystick under normal operating conditions that include both chair motion and volitional control is the sum of the feedthrough force and the force of volitional control. This is a reasonable assumption so long as the motion of the chair does not condition the attention or control abilities of the human.

This paper investigates the use of force reflection in the manual controls (joystick) to cancel feedthrough dynamics. An experimental apparatus was custom-built for the investigation by a team of students at Stanford University, with direction from Immersion Corporation. The apparatus consists of a single axis motion platform (chair) with an attached motorized joystick, as further described in Section 3

Our approach to counter feedthrough dynamics is fundamentally different to filtering approaches, which attempt to separate the feedthrough signals from the volitionally-produced signals using model-based filters. Although suppression of feedthrough dynamics has been demonstrated (Velger et al., 1988) (Idan and Merhav, 1989), we believe our more direct approach, which mechanically cancels the effect rather than electronically filters for it, will yield superior results. The greatest advantage of the new approach is expected to follow from the altered 'feel' of the joystick in the pilot's hand. In effect the pilot should feel as if he is manipulating the joystick in a Newtonian (fixed) reference frame rather than the accelerating frame of the vehicle. In addition, the force feedback approach will better maintain the joystick in the center of its kinematic workspace and will therefore avoid kinematic command saturation.

To begin the investigation, we develop a dynamical model of the pilot-vehicle system in Section 2. We assume a simple second order linear model for the pilot's arm and hand on the joystick. We estimate parameters to that model by fitting it to recorded data, collected using the motion platform in open-loop mode. This model-fitting algorithm is applied to two systems in Section 4: first a system with known parameter values, and then to a human subject's arm. Experiments on the closed loop system follow in Section 5. First, with the system of known parameter values in place, we demonstrate the existence of feedthrough dynamics. Then the previously fit model of the known system is used in a model-based compensator to cancel the feedthrough dynamics. Finally, we demonstrate and then cancel feedthrough dynamics with a human piloting the motion platform.

2 MODELING

In this section, we develop a lumped parameter model of the pilot-vehicle system to investigate the energetic interactions between pilot, joystick, and vehicle. We also develop a control block diagram to study the flow of information between pilot, joystick and vehicle. In this and the remaining sections, we assume that the human pilot exerts no volitional control.

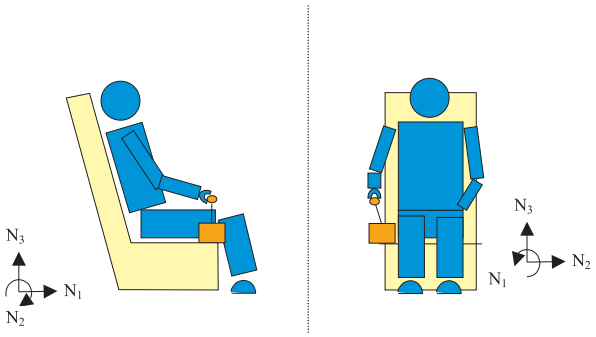

Figure 1. **Configuration of pilot, joystick and vehicle**

Figure 1 shows a pilot seated in a motion platform with one hand on a joystick. The pilot's torso is assumed fixed to the vehicle. The motion platform is assumed rigid, and the joystick base is rigidly mounted to the platform. The vehicle, joystick handle, and arm of the pilot are modeled as an articulated chain of rigid bodies, forming a closed loop. In the present study, a single axis motion platform is used, capable only of side-to-side motions, that is, parallel to unit vector $\mathbf{N}_2$. The joystick rotates about a horizontal axis parallel to unit vector $\mathbf{N}_1$. The hand, we assume, is linked to the joystick handle with a ball joint while the rest of the arm pivots about the elbow. The muscles are assumed to be in a state of steady activation, with the equilibrium position of the arm corresponding to the vertical orientation of the joystick.

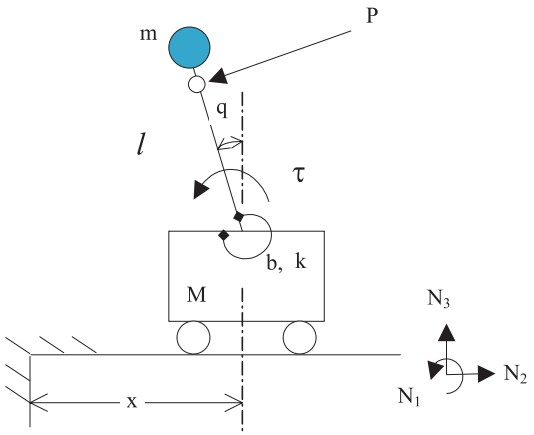

Figure 2. **Simplified model of the pilot, joystick, and vehicle**

Figure 2 shows a simplified system, incorporating additional assumptions. The linear displacement *x* locates the platform and

likewise the pivot of the joystick handle while the angular displacement q orients the joystick handle from the vertical. The first major modeling assumption involves representing the viscoelastic properties of the arm as a rotational spring and damper at the joystick pivot, with the equilibrium position of the spring at $q = 0$. The spring constant k and damping coefficient b account for the elastic and dissipative properties of both the joystick and the coupled human arm. The effective mass of the arm and the mass of the joystick handle are lumped in mass m located a distance l from the joystick pivot, while the mass of the chair and torso is M. The point P, located a distance r from the handle pivot, represents an attached linear accelerometer. A moment applied to the joystick of torque τ represents the joystick motor torque. In summary, the arm is modeled as a second order dynamical system, driven by the motion of the joystick base (x and its derivatives) and the joystick torque τ.

These modeling assumptions rest loosely on the results of a number of human subject experiments showing that the response of various human joints to mechanical excitation is approximately that of a linear second order system. (See, for example (Hajian and Howe, 1994)) Multimode models of the human body have been developed and tested for describing vibration feedthrough (Jex and Magdaleno, 1978). These models will be useful for refining the present work.

We are now in a position to write down the equations of motion for this system. The driving inputs we take to be the force acting on the platform and the torque acting on the joystick. The equations governing the motion of the pilot-vehicle system are:

$$\begin{aligned} ml^2\dot{u} - lm\cos(q)\dot{v} + bu + kq - mlg\sin(q) &= \tau \\ (m+M)\dot{v} - ml\dot{u}\cos(q) + mlu^2\sin(q) &= F \end{aligned} \tag{1}$$

where $u \triangleq \dot{q}$ and $v \triangleq \dot{x}$. We assume that the mass of the vehicle and the pilot's torso dominates the suspended mass of the pilot's arm and joystick handle, and that the acceleration of the platform accurately follows its command. In addition, we linearize about the operating point $q = 0$ and write the equations in state-space form

$$\dot{z} = Az + BU \tag{2}$$

using the following definitions:

$$\begin{aligned} A &= \begin{bmatrix} 0 & 1 \\ \frac{-k}{l^2m} + \frac{g}{l} & \frac{-b}{l^2m} \end{bmatrix}, \; B = \begin{bmatrix} 0 & 0 \\ \frac{1}{mL^2} & \frac{1}{lM} \end{bmatrix}, \\ z &= \begin{bmatrix} q \\ u \end{bmatrix}, \qquad U = \begin{bmatrix} \tau \\ F \end{bmatrix} \end{aligned} \tag{3}$$

This dynamical system is driven by the platform force F and joystick torque τ and responds with joystick angular displacement q and angular speed u. (The equations governing x and v have been rendered trivial by the assumptions and are not shown in Eq. (2).)

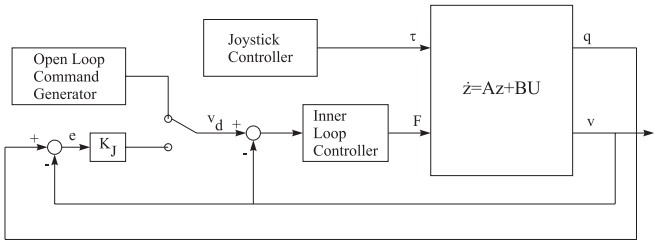

Figure 3. **Control Block Diagram**

Figure 3 shows this model as the plant in a block diagram with the vehicle control system. The joystick angular displacement q is fed back and interpreted as a setpoint for the platform speed. The measured platform speed $\dot{x}$ is subtracted from q to form the error e, which in turn is multiplied by the proportional gain K_J. Alternatively (as selected by a switch,) the system may be run open-loop, using a command generated independently by the host computer. A high gain inner loop in the motor controller is shown that ensures that the chair speed v closely tracks the desired speed v_d.

3 EXPERIMENTAL APPARATUS

Figure 4. **The Experimental Apparatus, showing the host computer, electronic cabinet, and motion platform with joystick**

Figure 4 shows the experimental apparatus. A welded aluminum frame rigidly supports a racing car seat and an Immer-

sion IE2000 powered joystick. Padded armrests are configured at elbow level while the joystick is mounted such that its handle may be comfortably grasped in the seated pilot's right hand. Joystick motion is restricted to rotation about an axis parallel to the armrest. The entire frame translates sideways on a ball screw assembly with a 0.45 m stroke. Translation is driven by a Brushless DC Servo Motor, rated at 3.4 kW. The motion platform is able to produce a sinusoidal motion of 2Hz with an amplitude up to A=0.10m, giving a peak acceleration $A\omega^2 = 16.11\, m/s^2 = 1.64$ g's.

4 OPEN LOOP EXPERIMENTS

In this section, we describe a set of open loop experiments intended to characterize the pilot's arm. The approach adopted here is to assume a simple lumped parameter model and estimate model parameters by fitting that model to recorded data. This model fitting procedure is developed and tested with a dummy arm in Section 4.1. Second, application of the fitting algorithm in a human subject experiment is described in Section 4.2.

The critical parameter is the effective mass of the pilot's arm, as seen at the joystick handle. In Section 5 below, the effective mass becomes a gain factor in the cancellation scheme. The mass m, however, is not available by observing excursions of the joystick to known platform accelerations since m appears as a coefficient on both $\dot{u}$ and $\dot{v}$ in Equation (1). Instead, we will use the data from two experiments to deduce the parameter m. The first is a dynamic experiment designed to estimate the natural frequency ω_n. The second is a quasi-static experiment designed to estimate the stiffness k. These two estimates are used together to arrive at the effective mass through the following formula, which follows from Equation (2):

$$m = \frac{k}{l^2(\omega_n^2 + g/l)}. \tag{4}$$

4.1 Model-Fitting Procedure

Before performing a model fitting experiment using a human subject, we applied the procedure to a mechanical model of a human arm, which we call the dummy arm. Figure 2 is suggestive of the mechanical form of the dummy arm. An assembly of weights is rigidly attached to the joystick handle to simulate the effective mass of the arm. An equivalent mass $m = 0.39$ kg with radius of gyration about the joystick pivot of $l = 0.16$ m was used. Rather than attaching a physical spring across the joystick pivot, a virtual spring was used. That is, the joystick motor was used to produce a torque proportional to the angular displacement with constant of proportionality $k = 0.23$ Nm/rad. No additional damping was used in the dummy beyond the inherent damping in the joystick.

A 32-bit interrupt-driven program running under DOS at a 333 Hz servo rate was developed to implement the joystick controller and the chair controller. Position encoders on the chair and joystick recorded chair displacement and joystick angle. An accelerometer was mounted to the platform to record $\dot{v}$. A linear accelerometer attached to the joystick handle at point P (See Figure 2) recorded acceleration of the joystick in the inertial reference frame of the earth, which we label $\ddot{y}$. To obtain the angular acceleration $\dot{u}$ from $\ddot{y}$, the following formula is applied to remove the component of gravity and account for the joystick angle:

$$\dot{u} = \frac{\dot{v}\cos(q) - \ddot{y} - g\sin(q)}{r} \tag{5}$$

A train of windowed pulses was used as the speed command to the platform, where an individual pulse is constructed from a full period of a cosine wave. A positive pulse and a negative pulse, both of period 0.3 seconds and amplitude $A = 0.15$ m/s alternate at intervals of 1.5 seconds. The dummy arm and joystick angular motion $[\dot{u}\ u\ q]$ were recorded. Figure 5 (d) shows the derivative of this speed command, the platform acceleration $\dot{v}$, as measured by an accelerometer. Figure 5 (a)-(c) shows the response of the dummy arm at the joystick.

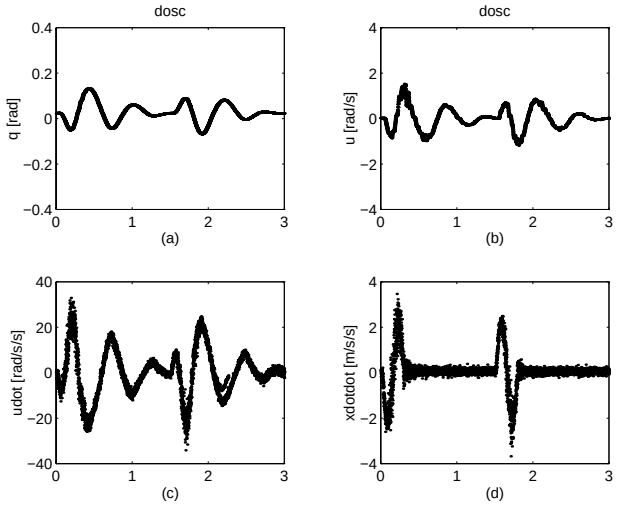

Figure 5. **Characterization data for dummy arm: (a) joystick angular displacement q (b) angular speed u, (c) angular acceleration $\dot{u}$, (d) platform acceleration $\dot{v}$. The x-axis is time in seconds.**

These data were fit with a model by least squares as follows.

Equation (2) may be used to express the platform acceleration $\dot{v}$ as the product of a matrix of motion values and a column

Table 1. Measured Parameter Values

$m = 0.39$	kg
$b = 0.6$	Nm/rad/s
$k = 0.23$	Nm/rad
$l = .16$	m
$g = 9.81$	m/s^2

vector of parameters in $Ax = b$ where

$$A = [\dot{u}\ u\ q],\ x = \begin{bmatrix} 1 \\ \frac{b}{ml^2} \\ \frac{k}{ml^2} - \frac{g}{l} \end{bmatrix},\ \text{and}\ \ b = \tfrac{1}{l}[\dot{v}]. \tag{6}$$

The data are arranged row-wise into the matrix A and vector b, respectively. Given n time-points of data, A is $(n \times 3)$ and b is $(n \times 1)$. The system $Ax = b$ then represents an over-determined set of equations for the parameter values in x. A pseudo-inverse of A may be used to solve for x:

$$x = (A^T A)^{-1} A^T b \tag{7}$$

The least-squares fit to the experimental data produced $x = [0.91\ 1.1\ 188]^T$. The fit natural frequency, in particular, corresponds to a period of 0.457 seconds. The actual parameter values are recorded in Table 4.1, per measurement or gain selection and calibration. The actual values correspond to a vector $x = [1.0\ 6.7\ 157]^T$

To extract a value for the effective mass, a value is required for the stiffness. Stiffness was characterized in a separate quasi-static experiment. A sinusoidally varying torque was commanded to the joystick while angular displacement was monitored. A linear least-squares fit yields a stiffness $k = 2.25$ Nm/rad.

The values for the natural frequency and stiffness combine to yield an effective mass

$$m = \frac{k}{l^2(\omega_n^2 + g/l)} = 0.34\,\text{kg} \tag{8}$$

This value compares favorably with the actual (measured) value $m = 0.39$ kg.

4.2 Characterization of a Human Arm

The dynamics of a human subject's arm were characterized using a procedure similar that applied above to the dummy arm.

Once again, Figure 6 (d) shows the derivative of the speed command, the platform acceleration $\dot{v}$, as measured by an accelerometer. Figure 6 (a)-(c) shows the response of the human arm at the joystick. The joystick angular displacement q, speed u, and acceleration $\dot{u}$ are shown in each of the subfigures. As in the characterization of the dummy arm in Section 4.1 above, the data of Figure 6 was used to determine the natural frequency of the feedthrough dynamics. The analysis yielded a parameter vector $x = [0.33\ -0.46\ 33]^T$.

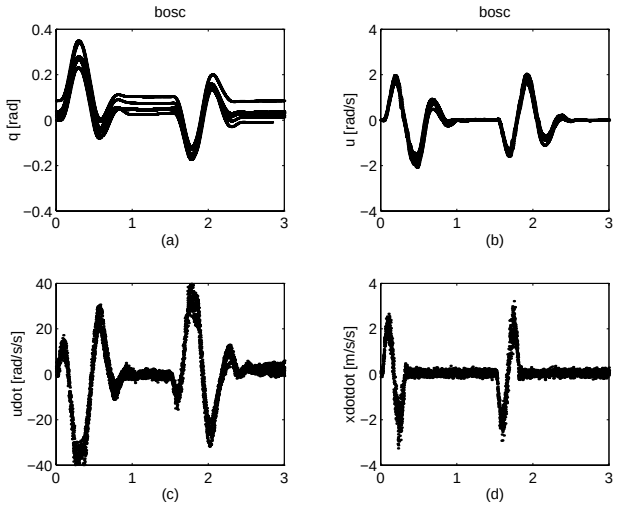

Figure 6. **Characterization data for human arm: (a) joystick angular displacement q (b) angular speed u, (c) angular acceleration $\dot{u}$, (d) platform acceleration $\dot{v}$. The x-axis is time in seconds.**

A sinusoidally varying torque was commanded to the joystick while angular displacement was monitored. A small virtual return spring ($K_J = -1.0$ Nm/rad) was also implemented on the joystick, so the stiffness observed is due to both the human arm and the virtual return spring. The slope of the line fit to the data produced $k = 1.88$ Nm/rad.

The values for the natural frequency and stiffness combine to yield an effective mass of $m = 0.75$ kg. This mass will be used as a gain factor in the canceling controller developed below.

We do not have a high confidence in the estimated effective mass of the human arm. In particular, the first value of the parameter vector should have been close to 1.0. Furthermore, the estimated natural frequency corresponds to a period of 1.08 seconds, which appears to be long compared to the period of oscillation seen in Figure 6.

5 CLOSED LOOP EXPERIMENTS

This section reports on experiments performed on the closed loop system, in which the displacements of the joystick are used as setpoints for the platform speed.

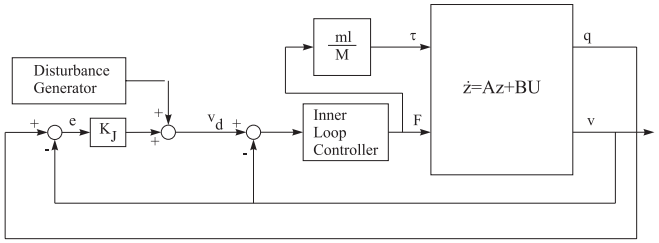

Figure 7. **Block diagram showing the feedthrough dynamics compensating controller.**

5.1 Feedthrough Dynamics Compensator

The feedthrough dynamics compensator is designed to produce a torque on the joystick that cancels the inertia force. The effective mass m of the arm and the acceleration of the platform are all that is needed of the model to compute the inertia force. The distance l of the effective mass m from the joystick pivot is used to compute the cancelling torque. The block diagram in Figure 7 shows the platform force F feeding forward with a gain factor ml/M to the joystick torque input. Also shown in the block diagram is the addition of a disturbance to the platform speed command.

5.2 Cancellation: Dummy Arm

We begin with a demonstration of the effects of the feedthrough dynamics of the dummy arm in the closed loop system. A negative gain $K = -0.6$ was used, so that joystick displacements to the left produced platform motion to the right and vice-versa. A speed command of the same profile used in the dynamic characterization experiments was added to the joystick setpoint as a disturbance. This disturbance was introduced to incite the dynamics, like a gust of wind acting on the body of a vehicle or a momentary roughness of terrain under the wheels. The disturbance acts only momentarily, for the short period $T = 0.3$ seconds. It does not feed energy into the interactive dynamics during the inter-disturbance intervals, which were 3.0 seconds (in contrast to the interval used for characterization: 1.5 seconds).

Figure 8 shows the effect of feedthrough dynamics on the dummy arm. Three periods of the motion are shown overlapped. In Figure 8 (d), the disturbance is recognized at $t = 0$ seconds, then the chair begins to accelerate back and forth with gradually increasing amplitude. The oscillations in the joystick angular displacement (Figure 8 (a)) are basically in phase with the platform accelerations (Figure 8 (d)), which corresponds to 180° out of phase considering the negative feedback gain $K = -0.6$. This figure clearly shows the unstable interactive dynamics.

Figure 9 shows the same closed-loop system of Figure 8 (with a feedback gain $K_J = -0.6$) but now with a feedforward gain (compensating controller gain) of $K_C = -0.15$. The closed loop dynamics are significantly altered. In particular, the unstable system oscillations have been stabilized. The same scales

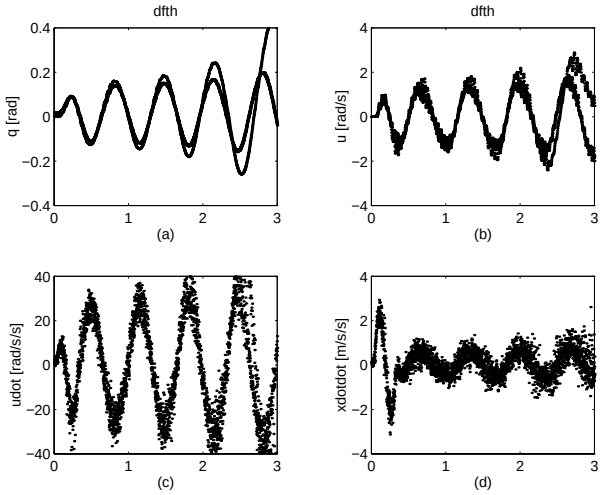

Figure 8. **Demonstration of the effects of feedthrough dynamics for the dummy arm: (a) joystick angular displacement q (b) angular speed u, (c) angular acceleration $\dot{u}$, (d) platform acceleration $\dot{v}$. The x-axis is time in seconds.**

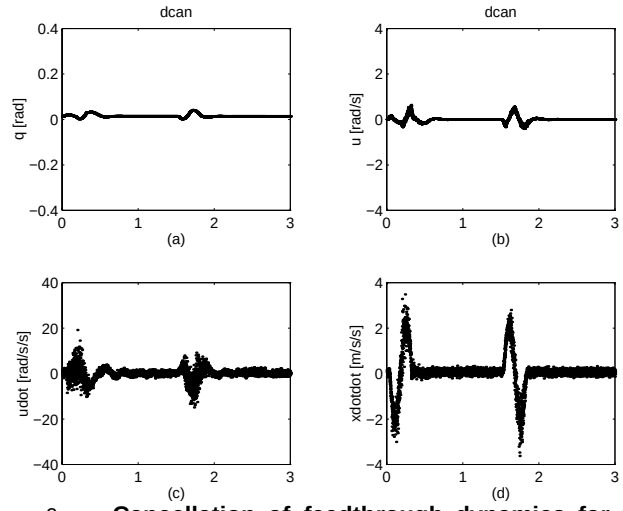

Figure 9. **Cancellation of feedthrough dynamics for the dummy arm: (a) joystick angular displacement q (b) angular speed u, (c) angular acceleration $\dot{u}$, (d) platform acceleration $\dot{v}$. The x-axis is time in seconds.**

are used in Figures 8 and 9, so that signal amplitudes may be directly compared. In contrast to Figure 8, however, two disturbance pulses appear in Figure 9 within the 3 second time interval recorded: one negative, and the second positive.

The feedforward gain $K_C = -0.15$ used to produce the plots above and chosen for its effectiveness during the experiment can now be compared to the gain recommended by our model-based design. The setup used for this experiment differed slightly from that used for the dummy model-fit above in that a larger

weight was used. The theoretical values are $m = 0.618$ kg and $l = 0.17$ m. A repeat model-fitting experiment yielded another very good fit to these new parameter values. The theoretical recommended feedforward gain, or multiplier on the platform acceleration [in m/s/s] to produce the torque is $K_C = lm = -0.10$. This number compares favorably to the gain used successfully.

5.3 Cancellation: Human Arm

The existence of the effects of feedthrough dynamics in a system closed through a human arm are first demonstrated. Thereafter, these effects are canceled using the same basic compensating controller used for the dummy arm. The signs of the feedback and feedforward gains, however, are reversed for the human arm. It was simply easier to generate the sustained oscillations using a positive feedback gain K_J for the human arm. This is probably due to the associated high stiffness and higher natural frequency of the human arm.

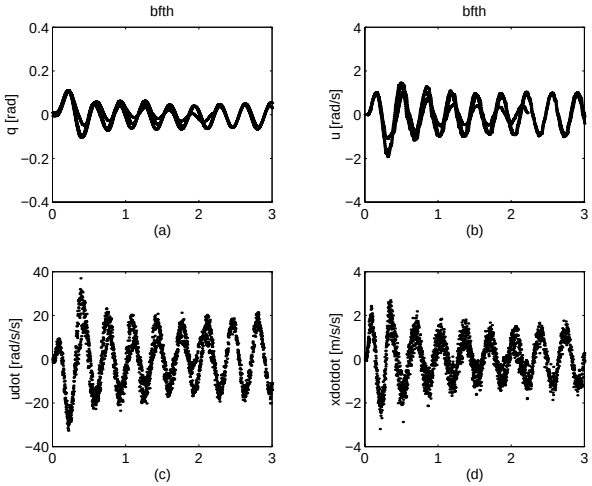

Figure 10. **Demonstration of Feedthrough Dynamics for a human arm (a) joystick angular displacement q (b) angular speed u, (c) angular acceleration $\dot{u}$, (d) platform acceleration $\dot{v}$. The x-axis is time in seconds.**

Figure 10 shows the response of the system closed around a human arm to the smoothed pulse-train stimulus with the interval of 3.0 seconds. The gain K_J had a value of 0.15 while $K_C = 0$. Thus only one pulse was applied during the 3 second trace shown. Three traces are shown overlapped in each subfigure. Again, the sustained oscillations are seen, this time barely stable.

Figure 11 shows the disturbance response of the closed loop system with the compensating controller in place. The feedback gain K_J still had a value of 0.15. But now a feedforward gain of $K_C = 0.16$ was used. Two impulses, one positive and the second negative were applied within the 6-second interval

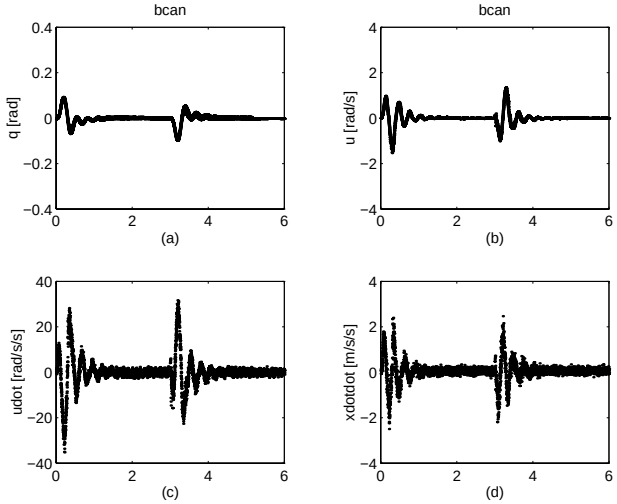

Figure 11. **Cancellation of feedthrough dynamics effect for the human arm. (a) joystick angular displacement q (b) angular speed u, (c) angular acceleration $\dot{u}$, (d) platform acceleration $\dot{v}$. The x-axis is time in seconds.**

shown. Although some oscillations were still present, they were well damped, diminishing to negligible amplitude in less than 1 second. The joystick torque output capabilities were saturating during this experiment, however. Total suppression of the feedthrough dynamics was not possible. Further work needs to be done with a powered joystick capable of higher torque output.

6 SUMMARY

The effects of feedthrough dynamics in a human-piloted vehicle were demonstrated. In particular, sustained oscillations in the closed loop system were shown to be due to accelerations of the vehicle "feeding through" the arm of the pilot to the joystick. The effects of feedthrough dynamics were reduced using a model-based feedforward controller. Using the feedforward controller, the oscillations present in the closed-loop system were quite effectively damped.

A simple second order model was assumed for the pilot's arm. A simple feedforward controller was designed on the notion of canceling the inertia force of the arm that results from accelerations of the vehicle. For this feedforward controller, an estimate of the effective mass of the arm as seen at the joystick is needed. To estimate a value for the effective mass , a set of experiments was designed. A dynamic experiment identified the natural frequency while a static experiment identified the stiffness. From these two, the effective mass was extracted. The entire procedure was first tested on a mechanical model of the human arm constructed by attaching a mass and a virtual spring to the joystick.

The entire approach adopted here, to cancel the effects of feedthrough dynamics by employing an additional control input

(the joystick torque,) is very promising. Especially in comparison to traditional approaches that involve model-based filtering of the control signal for spurious feedthrough-dynamic elements. Perhaps most interesting is that the pilot experiences a different behavior in the joystick and reports a different "feel". Although our results are only anecdotal, by current accounts the feel is improved. At present, it appears that our approach is in fact novel. In future work, a more complete control-theoretic treatment will be undertaken, including the introduction of more complete human dynamic models. In the present work, the most significant assumption in the model is the neglect of any voluntary effort on the part of the pilot. The human operators in our experiments were instructed to avoid voluntary effort. Future experiments will encompass voluntary effort in the model and the experiment. For example, performance at a tracking task will be monitored. We expect that this work will have direct implications for the long-standing tradeoff between vehicle stability and responsiveness, alleviating the need to compromise stability when responsiveness is increased.

Future work with the motion platform will also involve the development of an on-line system ID process. That is, when a new pilot sits down in the motion platform, an automated system ID procedure will be used to ascertain that pilot's feedthrough dynamic parameters. From these identified parameters, the force reflection control law can automatically be tuned.

7 ACKNOWLEDGEMENTS

The authors would like to thank the team at Stanford University who designed at built the motion platform: Michelle Johnson; Vinod Kumar Pabba; Gregory Clark; and Timothy Wang, and acknowledge the support of The Department of the Airforce through the SBIR grant "Commercially Viable Force Feedback Controllers, Phase II", awarded to Immersion Corporation.

REFERENCES

Banerjee, D., Jordan, M. L., and Rosen, M. J. (1996). Modeling the effects of inertial reactions on occupants of moving power wheelchairs. In *Proceedings, Rehabilitation Engg. and Assistive Tech. Soc. of North America*.

Hajian, A. Z. and Howe, R. D. (1994). Identification of the mechanical impedance of human fingers. In *Dynamic Systems and Controls*, volume 1 no. 55.

Idan, M. and Merhav, S. J. (1989). Effects of biodynamic coupling on the operator model. *Journal of Guidance*, 13(4):630–637.

Jex, H. R. and Magdaleno, R. E. (1978). Biomechanical models for vibration feedthrough to hands and head for a semisupine pilot. *Aviation, Space, and Environmental Medicine*, Biodynamics Symposium(XXVII):304–316.

Smith, J. W. and Montgomery, T. (1996). Biomechanically induced and controller coupled oscillations experienced on the F-16XL aircraft during rolling maneuvers. Technical Report 4752, NASA Technical Memorandum.

Velger, M., Grunwald, A., and Merhav, S. (1988). Adaptive filtering of biodynamic stick feedthrough in manipulation tasks on board moving platforms. *Journal of Guidance*, 11(2):153–158.